Journal of Nanoparticle Research (2006) 8:899–910
DOI 10.1007/s11051-005-9058-1

Nanocrystalline ruthenium oxide and ruthenium in sensing applications – an experimental and theoretical study

Anette Salomonsson[1], Rodrigo M. Petoral Jr.[2], Kajsa Uvdal[2], Christian Aulin[3], Per-Olov Käll[3], Lars Ojamäe[3], Michael Strand[4], Mehri Sanati[4] and Anita Lloyd Spetz[1,*]
[1]*S-SENCE and Division of Applied Physic, Linköping University, SE-581 83, Linköping, Sweden;* [2]*Division of Applied Physics and Sensor Science, Linköping University, SE-581 83, Linköping, Sweden;* [3]*Physical and Inorganic Chemistry, Linköping University, SE-581 83, Linköping, Sweden;* [4]*School of Technology and Design/Chemistry, Växjö University, SE-351 95, Växjö, Sweden; *Author for correspondence (Tel.: +46-13-281710; Fax: +46-13-288969; E-mail: spetz@ifm.liu.se)*

Received 10 June 2005; accepted in revised form 25 November 2005

Key words: nanoparticles, gas sensors, RuO_2, Ru, FET devices

Abstract

In this project, we have explored RuO_2 and Ru nanoparticles (~10 and ~5 nm, respectively, estimated from XRD data) to be used as gate material in field effect sensor devices. The particles were synthesized by wet chemical procedure. The capacitance versus voltage characteristics of the studied capacitance shifts to a lower voltage while exposed to reducing gases. The main objectives are to improve the selectivity of the FET sensors by tailoring the dimension and surface chemistry of the nanoparticles and to improve the high temperature stability. The sensors were characterized using capacitance versus voltage measurements, at different frequencies, 500 Hz to 1 MHz, and temperatures at 100–400°C. The sensor response patterns have been found to depend on operating temperature. X-ray photoelectron spectroscopy (XPS) analyses were performed to investigate the oxidation state due to gas exposure. Quantum-chemical computations suggest that heterolytic dissociative adsorption is favored and preliminary computations regarding water formation from adsorbed hydrogen and oxygen was also performed.

Introduction

Nanoparticles based on catalytic metal oxides have a very high surface area and new specific properties due to the small size and therefore they are interesting as gas sensing materials. Mostly resistivity changes due to gas exposure of the nanoparticle material is measured as the sensor response (Kolkamov et al., 2003; Vuong et al., 2005). In field effect devices like transistors or capacitors the nanoparticles are used as the gate material and polarization phenomena are detected (Salomonsson et al., 2005). Silicon carbide, SiC, as the semiconductor can be operated at a high temperature because of its wide bandgap (2.3 eV for the 4H polytype) and in corrosive environments due to the chemical inertness (Lloyd Spetz & Savage, 2003). The metal insulator SiC, MISiC, capacitor sensor with a catalytic gate material such as Pt is sensitive to reducing gases like hydrogen and hydrocarbons. The hydrogen-containing gases are decomposed on the catalytic metal surface and hydrogen atoms diffuse through the metal and adsorb on the insulator surface, see Figure 1 (Eriksson et al., 2005). It has been shown by DRIFT spectroscopy that OH groups forms on

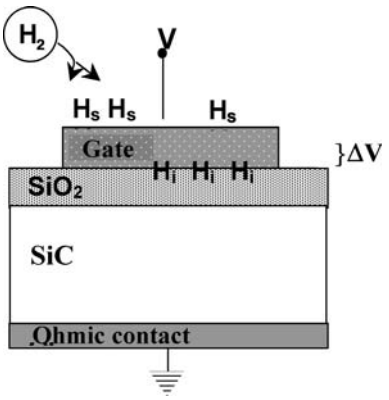

Figure 1. Schematic picture of the MISiC capacitor sensor. Dissociation of hydrogen on the gate contact and hydrogen atoms adsorbed on the insulator surface is indicated.

the surface of the insulator, which due to their strong dipole moment gives a polarization of the gate region in the device (Wallin et al., 2004, 2005). The polarization shifts the capacitance voltage curve to a lower voltage. The measured sensor signal is the voltage at a constant capacitance.

Sensitivity to ammonia requires a porous catalytic material. Triple points, that is sites on the sensor surface where both the catalytic metal and the insulator are in contact with the gas phase, are identified as necessary for the ammonia response (Löfdahl et al., 2001). Nanoparticles as gate material is expected to increase the number of triple phase boundaries and thereby the sensitivity.

Nanoparticles can be synthesized by a variety of techniques which have been reviewed earlier (Salomonsson et al., 2005). The particle size, shape and crystal structure can be designed to tailor make devices with special properties.

The gate material in a capacitor device has to conduct current. This put special requirements on the processing of the nanoparticles, e.g. the density of the particles has to be high enough and non-conducting particles have to be impregnated by metals.

In this work we have tested electrically conducting and catalytically active metal oxide particles of ruthenium dioxide (RuO_2). This material has been compared to nanoparticles of Ru in order to increase the knowledge of the sensing behavior of these materials. The RuO_2 shows promising redox properties and a high electronic conductivity (at RT: 35 μΩcm) that declines with temperature (Over, 2002). Other interesting material properties like high thermal stability and high resistance to chemical corrosion has been reviewed before (Salomonsson et al., 2005).

Ruthenium forms only one stable solid oxide phase, which is RuO_2. Oxides with higher oxidation number, RuO_3 and RuO_4 are volatile and toxic (Peden & Goodman, 1986), formed at oxidation temperature above 900°C. This limits the operation temperature of the sensors to temperatures below 650°C. In comparison metallic Ru is almost inactive in the catalytic oxidation of CO (Peden & Goodman, 1986), while RuO_2 is as active as metallic Pt (Böttcher et al., 1999; Wendt et al., 2002).

Studies made on Ru/β-SiC Schottky diodes (Roy et al., 2003) show that the sensor response to hydrogen improved with operating temperature, up to 400°C.

In this article, we report on ruthenium dioxide and ruthenium as gate material of MISiC field effect gas sensors. The sensitivity and stability of ruthenium dioxide and ruthenium as gate material was compared to platinum. The oxidation state was investigated by using XPS spectroscopy together with quantum-chemical computations. We discuss the sensor detection mechanism, and claim that even though resistive changes are present the main contribution to the output signal in RuO_2 and Ru MISiC sensors are based on field-effect changes.

Experimental section

Synthesizing of nanoparticles

A wet chemical method is used to synthesize particles of $RuCl_3{\cdot}xH_2O$ using 25% NH_3(aq) as the precipitate agent. The amorphous precursor of hydrated ruthenium oxide, "$Ru(OH)_3$", which is formed loses water upon heating. The crystallization process starts when nearly all the water has been removed at about 300°C (Málek et al., 1996).

The single-phase rutile RuO_2 nanoparticles obtained were examined by X-ray diffraction (XRD) (pure RuO_2 powder, no salt added), and the particle size was estimated to ~10 nm from Scherrer's equation. However, examination by transmission electron microscopy (TEM) indicated the true particle size to be about 20 nm (Figure 2).

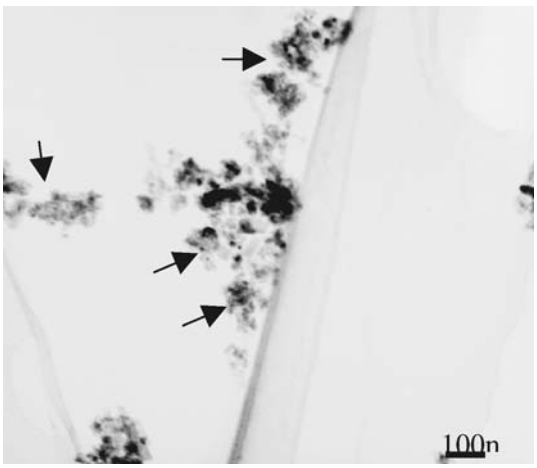

Figure 2. Representative TEM photograph of synthesized rutile-phase RuO_2 nanoparticles at 300°C.

In the synthesis of a nano-crystalline powder of metallic Ru tetraethylene glycol ($HOCH_2(CH_2OCH_2)_3CH_2OH$, TEG) was used as solvent. In the solution $RuCl_3{\cdot}xH_2O$ (0.20 g) and TEG, (20 ml) was dissolved and palmitic acid (0.49 g) was added as capping molecule. The suspension was heated to ~40°C.

Hydrogen peroxide (H_2O_2, 30%) 2 ml was then added slowly and in small portions to the solution and the temperature was increased to ~310°C under O_2-purge. During heating, the solution turned from dark red to dark green. Finally, a black precipitate was obtained, which was separated from the solvent by centrifugation and washed twice with deionized water. The XRD powder pattern (pure Ru material, average crystallite size of ~5 nm) showed a few broad intensities, all of which are attributable to metallic ruthenium (Figure 3).

Processing of the sensor gate

The sensors in this study were capacitors based on n-type 4H-SiC with RuO_2 or Ru as the gate material (Figure 1). The insulator consists of a thermal oxide of SiO_2 and a densified layer of Si_3N_4, with a top layer of SiO_x and a total thickness of 80 nm. Alloyed Ni with 5 nm $TaSi_x$ and 400 nm Pt as corrosion protection layer forms the ohmic rear contact to the SiC. A Ti/Pt layer on top of the sensor forms a bonding pad. The active gate region of Ru or RuO_2 was formed using a micro-

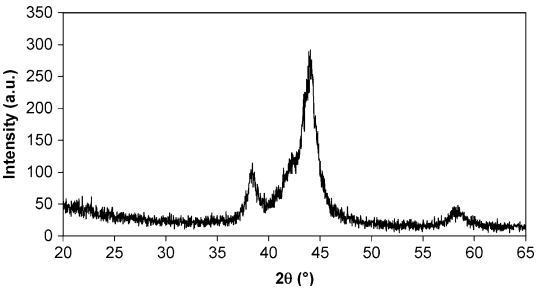

Figure 3. XRD pattern of the metallic Ru nanocrystals.

pipette for drop deposition of particles in a suspension of methanol and deionized water.

A constant volume (3 μl) of the suspension defines a gate area of ~1 mm diameter for each capacitor. Post-deposition annealing (400°C for 30 min) stabilizes the particles on the SiO_x surface and is also effective for consistent electrical behavior of the gate material.

Mounting and sensor testing

A Pt-100 element together with the sensor chip was glued onto a ceramic micro-heater and placed on a 16-pin holder (Figure 4). The Pt-100 element was used as temperature detector. For electric connections gold bonding are used.

The holders were mounted in leak tight aluminum capsules, which are connected to a gas flow line. The gases were primed across the sensor surfaces using a computer-controlled gas mixing system.

The electrical properties were evaluated using a Boonton 7200 capacitance meter and a Hewlett

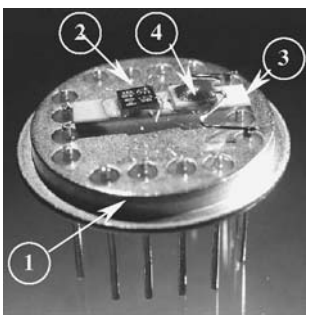

Figure 4. Mounting of the MISiC capacitor sensors, (1) 16-pin holder; (2) sensor chip; (3) ceramic heater; and (4) Pt-100 temperature detector.

Packard 41924 LF impedance analyzer. The capacitance–voltage (C(V)) characteristics were obtained at 500 kHz to 1 MHz. The C(V)-characteristic were first measured in synthetic air and thereafter in test gas mixtures.

Analysis and spectroscopic characterization

Mass spectrometer studies were carried out of the atmosphere in the vicinity of the sensors during gas exposure and operation of the sensors. In order to study the reaction products the gas flow before and after the sensors has been analyzed with a quadrupole residual gas analyzer (RGA). By using a capillary it is possible to reduce the pressure from atmospheric pressure in the reaction cell to 1×10^{-6} Torr in the mass spectrometer chamber.

XPS analysis was performed in a VG instrument with a CLAM2 analyzer and a twin Mg/Al anode. The pressure in the analysis chamber was approximately 5×10^{-10} mbar. The measurements were carried out with unmonochromated Mg Kα photons (1253.6 eV). The resolution was determined from the full width at half maximum (FWHM) of the Au($4f_{7/2}$) line, which was 1.3 eV with pass energy of 50 eV. The power of the X-ray source was kept constant at 300 W. The binding energy scale of the spectra was aligned through the Au($4f_{7/2}$) peak at 84 eV. Measurements were made using photoelectron take-off angles (TOA) of 30° and 80° with respect to the surface normal of the sample. The VGX900 data analysis software was used to calculate the elemental composition from the peak areas and to analyze the peak positions. Curve fitting is done using the program XPSPEAK version 4.1. To be able to study the effect of the exposed gases on RuO_2, the samples studied with XPS were prepared in the following way. One sample was held at 300°C in a 100 ml/min flow of 1% H_2 in N_2 for 6 h and the other sample was held at 300°C in a 100 ml/min flow of pure O_2 for 6 h. They were cooled down to room temperature (RT, 2 h, total time 8 h) keeping the same flow and composition of the gas and afterwards they were directly transported to the XPS chamber.

Theoretical modeling

The interaction of H_2, O_2 and NH_3 molecules with the RuO_2 surface was also investigated by quantum-chemical density functional theory (DFT) computations. The calculations were performed using the generalized-gradient functional PW91 (Perdew et al., 1992; White & Bird, 1994), ultra soft pseudo potentials (Vanderbilt, 1990) in combination with a plane wave basis set with a kinetic energy cut-off of 300 eV, and periodic boundary conditions, as implemented in the CASTEP program (Milman et al., 2000). The surface was mimicked in the calculations by a geometry-optimized two-layer surface slab cut along the (110) surface, where the surface unit cell consisted of 8 RuO_2 units. Similar computations have been used to study adsorption on ZnO (Persson et al., 2002) and TiO_2 (Ojamäe et al., 2005). These calculations are approximate, but still convey some understanding and rationalization for the molecular processes that give rise to the output signal.

Results

Electrical characterization and gas sensing properties

Two kinds of MISiC capacitors, with RuO_2 or Ru as the sensing material, were exposed to a series of test gases. The sensors show the same sensitivity pattern but with some pronounced small material related differences. The operation point is individual and differs from device to device, ~250 pF and ~150 pF is chosen for RuO_2 and Ru, respectively. The gate areas in these devices are not well defined due to the deposition method, which can explain the obtained result.

The C(V) curves were investigated at different frequencies in the range 500 Hz–1 MHz. Very similar results were obtained regarding accumulation and inversion capacitances as well as the gas induced voltage shift of the C(V) curves and only the 1 MHz results are presented here.

Characteristic shifts in the depletion region of the C(V) curves in synthetic air and hydrogen, respectively, are observed for RuO_2, and the shift increases as the temperature decreases (Figure 5a). The accumulation capacitance increases by temperature. For Ru the shift due to hydrogen gas shows a maximum at 300°C, while at 400°C it has totally disappeared (Figure 5b). This can at least partly be explained by changes of the surface composition since Ru starts to oxidize at temperatures above 200°C (Cocke et al., 1985).

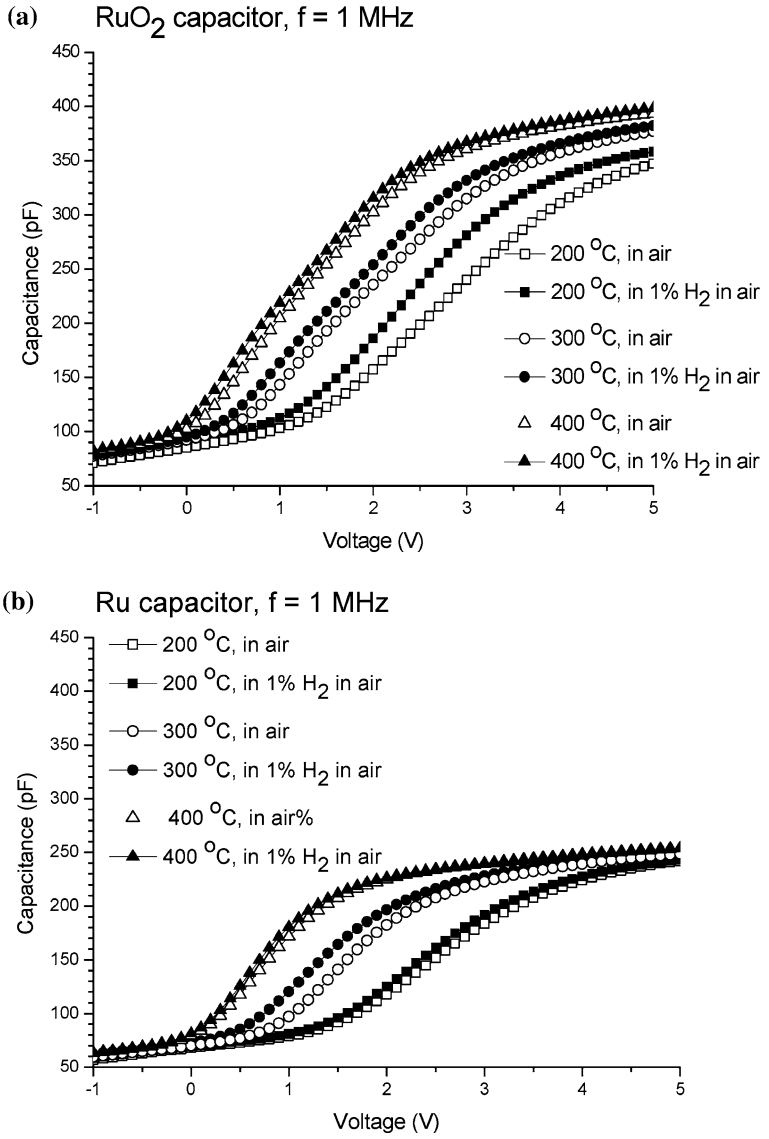

Figure 5. C(V) characteristics for (a) $RuO_2/SiO_x/Si_3N_4/SiO_2/SiC$ and (b) $Ru/SiO_x/Si_3N_4/SiO_2/SiC$ capacitors in synthetic air (open symbols) and 1% H_2 in synthetic air (filled symbols).

The voltage change at a constant capacitance to H_2, CO, C_3H_6 and NH_3 (all gases mixed with synthetic air) are compared (Figure 6a and b). The sensors show the same sensitivity pattern but a different temperature dependence, the latter is consistent with the shifts of the C(V)-curves (Figure 5). None of the sensors show any response to CO or NO, while both of them significantly respond to H_2, C_3H_6 and NH_3. The selectivity pattern with high response to hydrogen, ammonia and hydrocarbons (propene) is similar as for porous Pt and Ir gate MISiCFET devices (Lloyd & Savage, 2003; Andersson et al., 2004).

Changes in resistivity of the gate material, indicated from the change in accumulation capacitance by temperature, may contribute to the output signal, especially for RuO_2 (Figure 5a). It is possible that changes in oxidation state occur for both materials. The difference in selectivity at different operating temperature can be used in

arrays to detect several gas components in a mixture.

Mass spectrometer studies

The surface reactions on both RuO_2 and Ru during exposure to H_2 or NH_3 in air are studied with mass spectrometer. The desorption product from both active areas are mainly water. The data in Figure 7a–d, shows the water desorption together with the sensor response. The data shown are the differential spectra; the background water is withdrawn. Spectra with and without the sensor are recorded and then the differential of these measurements are plotted as the production of water from the sensor surface.

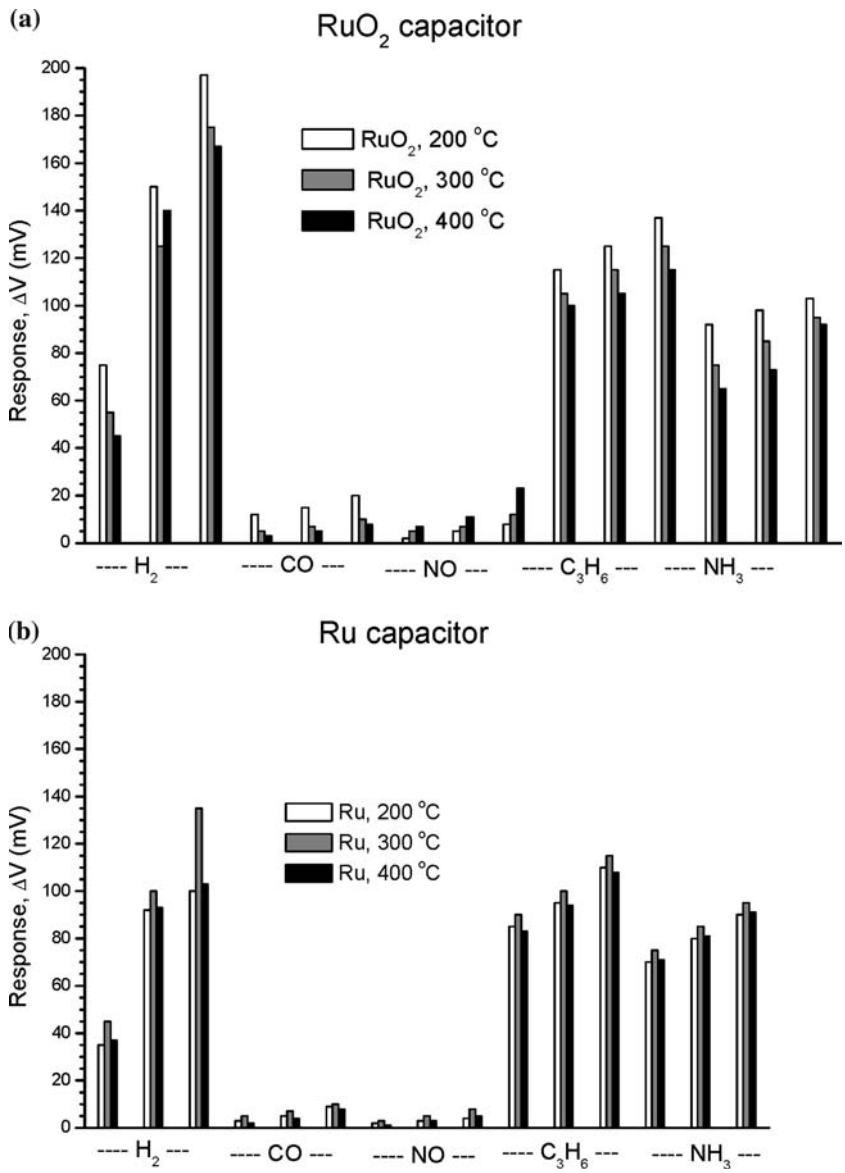

Figure 6. The gas response for (a) a RuO_2 capacitor, (b) a Ru capacitor (voltage shift at a constant capacitance) to 1000, 5000 and 1% H_2, 50, 100, 250, ppm CO or NO, 250, 500, 1000 ppm C_3H_6 and 250, 500, 1000 ppm NH_3. Carrier gas synthetic air.

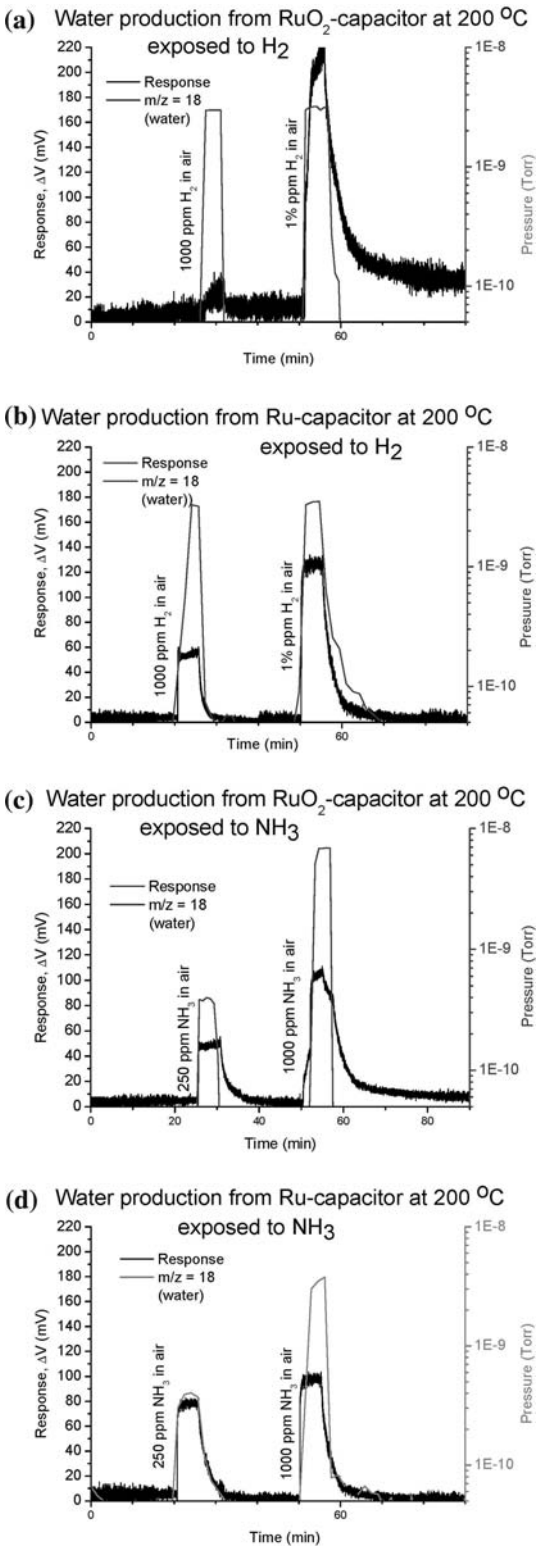

Figure 7. Mass spectrometer data of desorbed water ($m/z = 18$) when the sensors have been exposed to H_2 or NH_3 in synthetic air at 200°C. The sensors are (a) and (c) RuO_2 capacitor and (b) and (d) Ru capacitor.

For both RuO_2 and Ru the desorption of water during H_2 exposure (1000 ppm or 1% H_2 in synthetic air) is almost the same even though the H_2 concentration differs. The response to hydrogen of the sensors is however more pronounced for RuO_2 as the active material at the high hydrogen concentration while Ru is more sensitive for the lower concentration, see Figure 7a, b. In the case with NH_3 the difference in gas response between the two concentrations (250 or 1000 ppm NH_3 in synthetic air) is rather small for both materials, while the water production, contrary to the hydrogen case, show a large difference for the high and low concentration of ammonia, most pronounced for RuO_2, see Figure 7c, d. The different results for the hydrogen and the ammonia case are probably due to the difference in concentration of the gases. Other desorption products that were investigated were CO ($m/z = 28$), NO ($m/z = 30$), NO_2 ($m/z = 30$, $m/z = 46$), N_2O ($m/z = 44$, $m/z = 30$) and N_2O_2 ($m/z = 60$), as well as the test gases (H_2 and NH_3) in O_2/N_2 or N_2 ambient. However, only water gave a significant contribution.

XPS analysis

The Ru(3d) and Ru(3p) XPS core level spectra, measured at bulk mode (TOA = 30°), of RuO_2 nanoparticles heated at 300°C in presence of O_2 gas and then cooled down to room temperature are shown in Figures 8 and 9, respectively.

The Ru(3d), (Figure 8), core level spectrum consists of two main peaks at about 280.7 and 284.8 eV. The two peaks correspond to the 5/2 and 3/2 spin-orbit components of Ru (3d) with spin-orbit-splitting of about 4.1 eV, and is assigned to ruthenium oxide in the RuO_2. It is consistent with the peak positions and shape of RuO_2 thin films prepared when $RuCl_3$ aqueous solution is used as precursor material (Bhaskar et al., 2001; Rochefort et al., 2003). The binding energy position indicates a chemical state of ruthenium as rutile tetragonal RuO_2 (Bhaskar et al., 2001), which is consistent with the XRD results. Curve fitting of

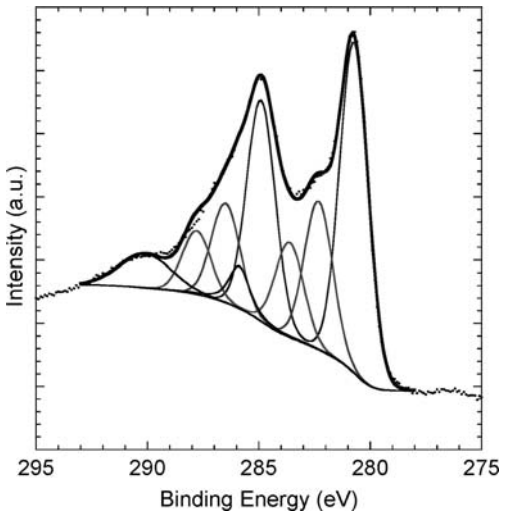

Figure 8. Ru(3d) XPS core level spectrum with two main peaks at 280.7 and 284.8 eV.

the spectra reveals the presence of higher binding energy contributions from Ru.

A doublet peak with binding energy (BE) at about 282.3 and 286.4 eV is assigned to the RuO_3 (Kim & Winograd, 1974) state while the doublet peak assigned to RuO_4 can be found at the binding energy position about 283.6 and 287.7 eV. It is possible that the presence of the high binding energy $Ru(3d_{5/2})$ core level peaks is due to the previously mentioned oxidation states of Ru according to some authors (Kim & Winograd, 1974). This mixed-valence interpretation has however been disputed by others (Cox et al., 1986). For them, the dominant low-binding energy spin-orbit doublet of RuO_2 is due to screened final state and higher binding energy doublets to unscreened final state. The interpretation is however consistent with the fact that RuO_3 is not known to be a stable phase. With the two conflicting ideas, we believe that in the as-synthesized RuO_2 nanoparticles, some high oxidation states still are present. As also suggested in literatures (Kim & Winograd, 1974; Iembo et al., 1997), the relatively rapid cooling process that the particle undergoes before XPS measurement (and even after the synthesis) probably enhances the formation of RuO_3 species.

Further curve fitting of the Ru(3d) narrow scan also reveals presence of by-products in the C(1s) region like alcohol/ether groups (~286 eV) and carbonyls/carboxyl group at a higher binding energy (~288–290 eV). The alcohol/ether groups may come from the solvent tetraethylene glycol while the carbonyls/carboxyls could come from the capping molecule that is the palmitic acid. Another by-product that is detected with the XPS measurement is the presence of a very small concentration (< 5%) of chlorine ($BE_{Cl\ 2p}$~198 eV). Chlorine may come from the unreacted $RuCl_3$. The peak corresponding to the $RuCl_3$ peak is expected to be seen at a BE ~281 eV in the Ru(3d) spectrum, but due to its minute concentration the peak may be overlapped by the RuO_2 main peak.

XPS narrow scan in the region of Ru(3p) is also conducted. A doublet peak having a BE of about 462.5 and 484.5 eV in the Ru(3p) core level spectrum (Figure 9) can be observed. The doublet corresponds to the spin-orbit splitting of Ru(3p) consistent with the RuO_2 chemical state. Curve fitting shows two more doublets present at higher binding energy positions. The two doublets binding energy positions are consistent with presence of RuO_3 and RuO_4 species. A peak present at about 475 eV may be due to inelastic scattering of the electrons.

Totally ~90% is Ru-related material and ~10% are carbon-containing by-products. The estimated amounts of the different types of ruthenium oxides in the as synthesized material based on XPS curve-fitting are as follows: RuO_2 (58%), RuO_3 (26%)

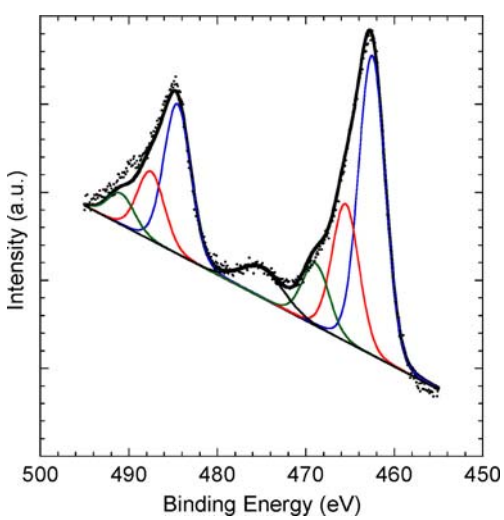

Figure 9. XPS narrow scan, here Ru(3p). A double peak having a BE of 462.5 and 484.5 eV can be observed.

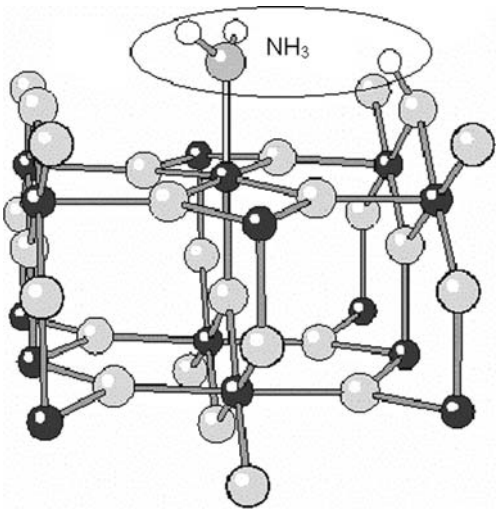

Figure 10. The structure of dissociated ammonia molecule chemisorbed at the RuO_2(110) surface as obtained from DFT computations. Black spheres represent Ru, gray oxygen, white hydrogen, and dark gray nitrogen (within the ellipse).

and RuO_4 (16%). Carbon-containing by-products are estimated to be less than 10% as calculated from the Ru(3d) narrow scan in Figure 8. It is worth noting that XPS measurement has also been done in a more surface sensitive mode (TOA = 80°). The shape of the surface mode spectra is similar to bulk mode results. The estimated amounts of the different oxides are also similar to the bulk.

For the RuO_2 nanoparticles with 1% H_2 exposure in presence of N_2 gas, the shape of the Ru(3d) spectra (figure not shown) is very similar to that of Figure 8. There is almost no change in the shape of the $Ru(3d_{5/2})$ and $Ru(3d_{3/2})$ core level peaks upon H_2 exposure (in nitrogen) which indicates that (irreversible) permanent surface reduction of RuO_2 does not occur. Also there is no decrease in the intensity of higher binding energy doublet peaks which would have indicated that the reduction of the oxide (RuO_2) has occurred upon H_2 exposure. The shape of the surface mode spectra is similar to the bulk mode spectra. The different ruthenium oxide polymorphs after exposure to 1% H_2 in N_2 are the following: RuO_2 (57%), RuO_3 (26%) and RuO_4 (17%). Carbon-containing by-products is estimated to be about 15% estimated from the Ru(3d) spectrum.

Computational calculations

From the quantum-chemical computations the H_2 molecule was found to adsorb in a tilted configuration on top of the surface of Ru ions that lack full coordination, with the rather high adsorption energy 0.52 eV. This is essentially in agreement with earlier DFT studies (Wang et al., 2003), although the H_2 adsorption energy is somewhat overestimated in the present study (this may e.g. be due to different functional being used or to the slab being thinner in the present study). If the H_2 molecule is assumed to bind dissociatively to the surface through a heterolytic reaction where one H^+ is transferred to a bridging surface oxygen atom while an H^- is transferred to the Ru ion, the adsorption energy is increased to 1.04 eV. Also the case where homolytic dissociation into two H^+ that are transferred to a bridging oxygen ion (thereby effectively forming a water molecule bound to an oxygen vacancy) and two electrons that will reduce two Ru ions was tested: this process was found to be slightly endothermic by 0.03 eV. According to the present calculations, heterolytic dissociative adsorption is thus thermodynamically favored.

The ammonia molecule was found to adsorb through N to the surface Ru ion, with the adsorption energy 1.60 eV. A dissociative binding mode where a proton has been transferred to a surface oxygen ion (Figure 10) was calculated to have adsorption energy of 0.63 eV, implying that the dissociation reaction of ammonia from the gaseous state is an exothermic process, although the dissociation reaction of already adsorbed ammonia will be endothermic.

Some preliminary computations regarding the formation of H_2O from H_2 and O_2 were also performed. The reaction energy for the following reaction was calculated to be 1.0 eV:

$$H_2(g) + RuO_2(s) \rightarrow H_2O(g) + RuO_2[\text{O surface vacancy}](s) \quad (1)$$

where (g) symbolizes the gas phase and (s) the surface.

This reaction creates a surface oxygen vacancy: one could possibly envision that the vacancy would contribute to the mechanism of further water production.

The adsorption energy of an O_2 molecule at this vacancy was 2.2 eV. The reaction of H_2 with this defect structure,

$$H_2(g) + O_2 \cdot RuO_2[\text{O surface vacancy}](s) \rightarrow H_2O(g) + RuO_2(s) \quad (2)$$

has a reaction energy $\Delta E = 3.7$ eV, and is thus highly exothermic. This hints to a possible decomposition reaction path to explain the high sensitivity observed for H_2 detection. The feasibility of such a mechanism will actually depend on the transition state energies present, which have not been calculated here and are awaiting future studies.

Discussion

RuO_2 is interesting as gate material in MISiCFET sensors since the material is conducting although it is an oxide. Most metal oxides well known as gas sensing materials (TiO_2, SnO_3...) do not have this feature. By using RuO_2 as the active layer we expected a selectivity pattern different from gas sensors where the active materials are metal films (Salomonsson et al., 2005). In this paper we have compared the results to sensors with Ru particles as the sensing material. RuO_2 as compared to Ru or e.g. Pt has the potential to be more long-term stable since the formation of an oxide, which may be one reason for drift, already has taken place. The result of the sensitivity to different gases of RuO_2 and Ru in Figure 7 indicates a higher catalytic activity for RuO_2 as compared to Ru. While the heat of adsorption of O_2 and H_2 decreases from left to right in the periodic table, the catalytic reaction rates peak at the transition metals (Re, Os, Ir, Pt, Au). For instance, to some extent, higher temperature is needed to exhibit sensitivity towards ammonia (for ammonia detection) when Ir is used as a sensing material on MISiCFET-gas sensors as compared to platinum (Andersson et al., 2004). A Pt surface was shown to have a higher hydroxyl formation rate as compared to Pd during hydrogen/Oxygen exposure (Löfdahl et al., 2002). Ru is reported to have the lowest catalytic activity towards H_2 among the transition metals while RuO_2 turns out to be as active as Pt, Rh and Pd (Over & Muhler, 2003), in agreement with the result in Figure 6a, b where the maximum sensitivity for Ru occurs at a somewhat higher temperature, 300°C. This different behavior of the sensors can be related to different catalytic activity of the gate materials.

For MOS capacitor devices a conducting gate contact is required. The nanoparticles of RuO_2 and Ru are based on conducting material but the drop-deposition method sometimes gives a too low density of the nanoparticles, which probably is the reason for the difference (at different temperature) in accumulation capacitance in Figure 5a. Therefore the C(V) characteristics were tested at different frequencies, since gate contacts with a low conductivity normally perform better in C(V) measurements at a lower frequency. However, the lower frequency did not show any impact on the results.

The XPS data confirmed the XRD results, that the rutile form of RuO_2 has been synthesized. The results also indicate the presence of some higher oxidation state material (RuO_2 58%, RuO_3 28%, RuO_4 16%). The XPS results also suggest that traces of contamination less than 10%, from the solvent as well as the capping molecules exist. From XPS analysis no conclusions about oxidation and reduction of the material due to gas exposure can be drawn. There is no decrease in the intensity of higher binding energy doublet corresponding to higher oxidation states of Ru which would have indicated that the reduction of the oxide (RuO_2) has occurred upon H_2 exposure. It would have been interesting to record spectra during the gas exposure but this is not technically possible in this system. Synchrotron studies could eventually give further information.

The modeling suggests heterolytic dissociation of hydrogen where H^- adsorbs on Ru and H^+ is transferred to a neighboring oxygen atom. For NH_3 molecules the calculations suggest that dissociative adsorption from the gas phase occur where NH_2 adsorbs on an Ru atom and H forms an OH group with a bridging oxygen atom. We refer to the much studied detection mechanism of hydrogen and ammonia in devices with a porous catalytic metal on a SiO_2 surface (Löfdahl et al., 2001; Åbom et al., 2003; Wallin et al., 2004, 2005). It is interesting to compare the mechanism where e.g. a hydrogen atom or proton from dissociated hydrogen or ammonia is transferred from the metal to the insulator to the mechanism on the RuO_2 surface. This means that the Ru–O site is compared to a triple point, described in the Introduction.

On Pd-MOS devices the ammonia dissociation is shown to be promoted by oxygen (Fogelberg et al., 1987). Experimentally it is shown that when an oxygen covered metal surface is exposed to ammonia the ammonia will dissociate and the released hydrogen will react with adsorbed oxygen to form water, which will desorb. Experimental evidence, e.g. from Diffuse Reflectance Infrared Fourier Transform (DRIFT) spectroscopy, exist which shows that even in an oxygen ambient ammonia dissociates at the triple points (metal, oxide, gas), in such a way that hydrogen is released to the oxide and there forms hydroxyl groups on the oxide (Löfdahl et al., 2002; Wallin et al., 2004, 2005).

The modeling also indicates that oxygen vacancies may provide an important reaction path for the water production. A H_2 molecule is assumed in the modeling to bind dissociatively to the surface, where one H^+ is transferred to bridging surface oxygen while an H^- is transferred to the Ru ion. The formation of water on RuO_2 creates surface oxygen vacancies were the O_2 can adsorb and in this way even more H_2 can adsorb and the reaction rate of water formation is increased. This should however be further studied by DRIFT-spectroscopy.

By combining different types of conducting and non-conducting oxides a more selective material could be designed. Proper mixing of the materials may produce a stabilizing matrix for increased long-term stability of the devices.

Conclusions

Conducting metal oxide nanoparticles are potential candidates as active gate material in MISiC capacitors. Chemically synthesized ruthenium oxide or ruthenium nanoparticles as gate material exhibit sensitivity to hydrogen containing gas molecules. The sensitivity pattern depends on the operating temperature and the optimum value of the sensor response was obtained for RuO_2 at 200°C and for Ru at 300°C. This is consistent with the catalytic activity e.g. for the water production of these materials.

The RuO_2 material due to the oxidized state has the potential of a very stable gate material for FET sensors for detection of gases like H_2, NH_3, HC at medium high temperature (200–300°C).

Preadsorbed oxygen together with oxygen vacancies are identified by theoretical modeling as important parameters in the mechanism for the water production. The use of a metal oxide as gate material give interesting suggestion for the detection mechanism through the comparison to porous metals as gate material on SiO_2.

Acknowledgements

This work was supported by grants from the Swedish Research Council, the Swedish Agency for Innovation Systems and Swedish Industry through the Center of Excellence, S-SENCE. We would like to thank Jeanette Nilsson for deposition of contact metals, and Evald Mild, at Linköping University, Sweden, who performed the skillful mounting of the sensor chips.

References

Andersson M., P. Ljung, M. Mattson, M. Löfdahl & A. Lloyd Spetz, 2004. Investigations on the possibilities of a MISiC-FET sensor system for OBD and combustion control utilizing different catalytic gate materials. Topics Catal. 30/31, 365.

Åbom A.E., E. Comini, G. Sberveglieri, N. Finnegan, I. Petrov, L. Hultman & M. Eriksson, 2003. Experimental evidence for a dissociation mechanism in NH_3 detection with MIS field-effect devices. Sensors Actuators B 89, 1–8.

Bhaskar S., P.S. Dobal, S.B. Majumder & R.S. Katiyar, 2001. X-ray photoelectron spectroscopy and micro-Raman analysis of conductive RuO_2 thin films. J. Appl. Phys. 89, 2987–2992.

Böttcher A., M. Rogozia, H. Niehus, H. Over & G. Ertl, 1999. Transient experiments on CO_2 formation by the CO oxidation reaction over oxygen-rich Ru(0001) surfaces. J. Phys. Chem. B 103, 6267–6271.

Cocke D.L., G. Abend, J.H. Block & N. Kruse, 1985. Oxidation of ruthenium studied by pulsed field desorption mass spectrometry. Langmuir 1, 507–509.

Cox P.A., J.B. Goodenough, P.J. Tavener, D. Telles & R.G. Egdell, 1986. The electronic structure of $Bi_{2-x}Gd_xRu_2O_7$ and RuO_2: a study by electron spectroscopy. J. Solid State Chem. 62, 360–370.

Eriksson M., A. Salomonsson, I. Lundström, D. Briand & A.E. Åbom, 2005. The influence of the insulator surface properties on the hydrogen response of field-effect gas sensors. J. Appl. Phys. 98, 034903-1–034903-6.

Fogelberg J., I. Lundström & L.-G. Petersson, 1987. Ammonia dissociation on oxygen covered palladium studied with a hydrogen sensitive Pd-MOS device. Phys. Scripta 35, 702–705.

Iembo A., F. Fuso, E. Arimondo, C. Ciofi, G. Pennelli, G.M. Curro, F. Neri & M. Allegrini, 1997. Pulsed laser deposition and characterization of conductive RuO_2 thin films. J. Mater. Res. 12, 1433–1436.

Kim K.S. & N.J. Winograd, 1974. X-ray photoelectron spectroscopic studies of ruthenium-oxygen surfaces. J. Catal. 35, 66–72.

Kolkamov A., Y. Zhang, G. Cheng & M. Moskovits, 2003. Detection of CO and O_2 using tin oxide nanowire sensors. Adv. Mater. 15(12), 997–1000.

Lloyd Spetz A. & S. Savage, 2003. Advances in FET chemical gas sensors. In: Choyke W.J., Matsunami H. and Pensl G. eds. Recent Major Advances in SiC. Springer, Berlin, pp. 879–906.

Löfdahl M., C. Utaiwasin, A. Carlsson, I. Lundström & M. Eriksson, 2001. Gas response dependence on gate metal morphology of field-effect devices. Sensors Actuators B 80, 183–192.

Löfdahl M., M. Eriksson, M. Johansson & I. Lundström, 2002. Difference in hydrogen sensitivity between Pt and Pd field-effect devices. J. Appl. Phys. 91, 4275–4280.

Málek J., A. Watanabe & T. Mitsuhashi, 1996. Crystallization kinetics of amorphous RuO_2. Thermochim. Acta 282/283, 131–142.

Milman V., B. Winkler, J.A. White, C.J. Pickard, M.C. Payne, E.V. Akhmatskaya & R.H. Nobes, 2000. Electronic structure, properties and phase stability of inorganic crystals: A pseudopotential plane-wave study. Int. J. Quantum Chem. 77(5), 895–910.

Ojamäe, L., C. Aulin, H. Pedersen & P.-O. Käll, 2005. IR and quantum-chemical studies of carboxylic acid and glycine adsorption on rutile TiO_2 nanoparticles. J. Colloid Interface Sci. (in press).

Over H., 2002. Ruthenium dioxide, a fascinating material for atomic scale surface chemistry. Appl. Phys. A 75, 37–44.

Over H. & M. Muhler, 2003. Catalytic CO oxidation over ruthenium-bridging the pressure gap. Prog. Surf. Sci. 72, 3–17.

Persson P., S. Lunell & L. Ojamäe, 2002. Quantum chemical prediction of the adsorption conformations and dynamics at HCOOH-covered ZnO(100) surfaces. Int. J. Quantum Chem. 89, 172–180.

Peden C.H.F. & D.W. Goodman, 1986. Kinetics of CO oxidation over Ru(0001). J. Phys. Chem. 90, 1360–1365.

Perdew J.P., J.A. Chevary, S.H. Vosko, K.A. Jackson, M.R. Pederson, D.J. Singh & C. Fiolhais, 1992. Phys. Rev. B 46(11), 6671–6687.

Rochefort D., P. Dabo, D. Guay & P.M.A. Sherwood, 2003. XPS investigations of thermally prepared RuO_2 electrodes in reductive conditions. Electrochim. Acta 48, 4245–4252.

Roy S., C. Jacob, C. Lang & S. Basu, 2003. Studies on Ru/3C-SiC Schottky junctions for high temperature hydrogen sensors. J. Electrochem. Soc. 150(6), H135–H139.

Salomonsson A., S. Roy, C. Aulin, J. Cerdà, P.-O. Käll, L. Ojamäe, M. Strand, M. Sanati & A. Lloyd Spetz, 2005. Nanoparticles for long-term stable, more selective MI-SiCFEt gas sensors. Sensors Actuators B 107(2), 831–838.

Vanderbilt D., 1990. Soft self-consistent pseudopotentials in a generalized eigenvalue formalism. Phys. Rev. B 41(11), 7892–7895.

Vuong D.D., G. Sakai, K. Shimanoe & N. Yamazoe, 2005. Hydrogen sulfide gas sensing properties of thin films derived from SnO_2 sols different in grain size. Sensors Actuators B 105, 437–442.

Wallin M., H. Grönbeck, A. Lloyd Spetz & M. Skoglundh, 2004. Vibrational study of ammonia adsorption on Pt/SiO_2. Appl. Surf. Sci. 235, 487.

Wallin M., H. Grönbeck, A. Lloyd Spetz, M. Eriksson & M. Skoglundh, 2005. Vibrational analysis of H_2 and D_2 adsorption on Pt/SiO_2. J. Phys. Chem. B 109, 9581–9588.

Wang J., C.Y. Fan, Q. Sun, K. Reuter, K. Jacobi, M. Scheffler & G. Ertl, 2003. Surface coordination chemistry: dihydrogen versus hydride complexes on RuO_2(110). Angew. Chem. Int. Ed. 42(19), 2151–2154.

Wendt S., A.P. Seitsonen, Y.D. Kim, M. Knapp, H. Idriss & H. Over, 2002. Complex redox chemistry on the RuO2(110) surface: experiment and theory. Surf. Sci. 505, 137–152.

White J.A. & D.M. Bird, 1994. Implementation of gradient-corrected exchange-correlation potentials in Car-Parrinello total-energy calculations. Phys. Rev. B 50, 4954–4957.